



STUDY ON THE LOW TEMPERATURE OPERABILITY IMPROVEMENT OF THE HEAT PUMP DRYER USING A SOLAR COLLECTOR AND AN AIR COLLECTOR

I. S. Hwang and Y. L. Lee

Department of Mechanical Engineering, Kongju National University, Korea

E-Mail: ylee@kongju.ac.kr

ABSTRACT

When drying frozen materials using a heat pump dryer, frost is formed on the evaporator, resulting in the liquid flood back of the compressor. Therefore, in this paper, a numerical analysis was conducted of a heat pump dryer with attached solar collector and air collector in order to enhance the low temperature performance of the heat pump dryer. According to the analysis results, when the solar collector was used in the given conditions, the low temperature performance was improved through the increase of evaporating pressure by approximately 61 kPa. Also, the COP increased by a maximum of 1.5 compared to the standard cycle. Meanwhile, when using the air collector, the evaporating pressure increased by 209 kPa and the COP increased by a maximum of 5.5 over the standard cycle. Thus, it is found that the air collector is more effective than the solar collector in the considered conditions.

Keywords: heat pump dryer, solar collector, air collector, condensation.

INTRODUCTION

Drying refers to the separation and removal of humidity and moisture from a material. In order to increase the drying speed, the surrounding temperature has to be increased, the humidity lowered, and the surroundings have to be well ventilated. Methods of drying can be largely divided into the high temperature hot air drying method using an electric heater or gas, and the drying method using a heat pump.

The drying method using high temperature hot air involves high temperature air penetrating the drying material to become humid air. This high temperature humid air is not effective in the drying process and is frequently expelled to the outside. However, if the heat of the expelled high temperature humid air is retrieved, it will contribute to improving efficiency and the drying process.

The heat pump dryer is mainly composed of a compressor, a condenser, an expansion valve and an evaporator. An evaporator and a condenser are attached within the drying chamber. The drying process of the heat pump dryer involves dry air passing through the condenser to have its temperature increased and humidity reduced, then penetrating the drying material, which results in its increase in humidity before entering the evaporator to undergo dehumidification, lowering the humidity of the air. High temperature humid air passes through the evaporator to become dry air of relatively low temperature and the heat in the air at this time is retrieved through the evaporator, resulting in higher efficiency in comparison to dryers of other methods.

The heat pump dryer has been used for wood and food drying since the 1970s [1], and various studies on it have been conducted. Prasertsan *et al.*, [2] investigated the effect of heat pump operation conditions on the drying rate, and Bivens *et al.*, [3] applied an internal heat exchanger which improved the heat pump dryer performance by approximately 6 - 7%. Cho *et al.*, [4] verified experimentally that applying the internal heat

exchanger results in the heat pump cycle performance of approximately 9%. Sarkar *et al.*, [5] examined through simulation the relationship between the optimum compressor discharge pressure and performance according to the refrigerant type, and Baek *et al.*, [6, 7] conducted simultaneous theoretical analysis and experimental study regarding the cycle with a piston-cylinder shape expander applied. It was found that by using a heat pump supported with solar heat, the COP increased significantly and was effective as an auxiliary heat source during the winter time.

Also, many studies are currently being conducted regarding the use of external heat sources, including geothermal heat and waste heat, in addition to the solar heat assisted heat pump [8, 9]. Using an external heat source provides an increase in performance of the heat pump dryer, as well as its low temperature performance during the winter time, or when drying a frozen material.

Therefore, in this paper, a solar collector and an air collector were used as an auxiliary evaporator to improve the operability of the heat pump dryer at low temperature as well as the efficiency of the dryer. To do this, the performance of the heat pump dryer with the solar collector and air collector were analyzed using cycle analysis. Moreover, CFD (Computational Fluid Dynamics) was utilized to perform performance analysis of the solar collector.

Analysis method and conditions

Before analyzing the cycle with the solar collector applied, the heat exchange performance of the solar collector was analyzed according to the amount of solar irradiation. Figure-1 shows the computational domain of the solar collector. In order to reduce the analysis time, 1 out of the 9 solar collector modules was selected to conduct 1/9 modeling of the entire model. As shown in Figure-2, the 1/9 model was composed of an absorber plate of length 1800 mm, width 100 mm, and



thickness 2 mm and a pipe of diameter 9 mm. On the top surface of the absorber plate, heat fluxes of 1000W/m^2 for summer and 600W/m^2 for winter were assumed and the other side was assumed to be insulated.

Figure-3 shows the schematic diagram of the solar collector and air collector attached to the standard cycle dryer. A plate-type heat exchanger was attached between the expansion valve and evaporator to allow heat exchange between the warmed hot water and refrigerant through the solar collector. Also, the air collector was installed outside the drying chamber to inject heat from the outside into the drying chamber.

Analysis using EES was performed in order to investigate the low temperature operation performance and cycle variation of the solar collector and air collector using the heat pump dryer. The compressor used for the cycle analysis was of the scroll type with a stroke volume of $2.9 \times 10^{-3} \text{ m}^3/\text{s}$ and the compressor efficiency was assumed to be 0.55. Meanwhile, the total amount of heat transferred from the evaporator was simplified as shown in equation (1). Here, α is the multiplication of the evaporator effectiveness, mass flow rate of the air passing through the evaporator, and the specific heat of the passing air, and α was assumed to be 0.5 kW/K . Also, the transferred total amount of heat from the condenser was simplified as shown in equation (2) and β was assumed to have the value of 0.5 kW/K .

$$Q_{\text{evap}} = \alpha(T_{\text{sat, evap}} - T_{\text{air, evap}})$$

$$= \epsilon \dot{m}_{\text{air, evap}} C_{\text{air, evap}} (T_{\text{sat, evap}} - T_{\text{air, evap}}) \quad (1)$$

$$Q_{\text{cond}} = \beta(T_{\text{sat, cond}} - T_{\text{air, cond}})$$

$$= \epsilon \dot{m}_{\text{air, cond}} C_{\text{air, cond}} (T_{\text{sat, cond}} - T_{\text{air, cond}}) \quad (2)$$

Conduction analysis was performed to predict the condensation and frost on the air collector fin. Figure-4 shows the air collector conduction analysis model. Analysis was conducted on one module of the air collector, and the modeling used the dimensions of $W=22 \text{ mm}$, $L=26 \text{ mm}$, and $D=10 \text{ mm}$ with a fin pitch of 4.2 mm . The inner tube evaporating temperature was assumed, the surface in contact with the outside air was assumed to have an air temperature 10°C , and the convective heat transfer coefficient was assumed to be $10 - 30 \text{ W/m}^2\text{K}$.

RESULTS AND DISCUSSIONS

Solar collector performance analysis

Before performing the cycle analysis of the heat pump dryer with the solar collector, CFD was used to predict the variation of heat absorption of the solar collector with solar irradiation. Figure-5 shows the solar collector absorption heat and temperature difference

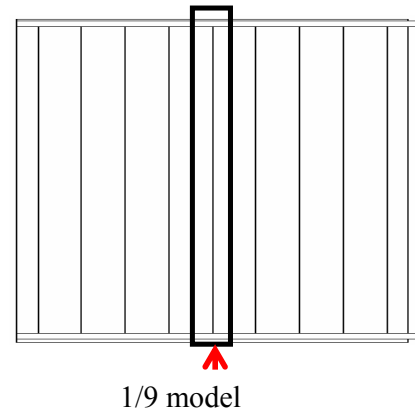


Figure-1. Computational domain of the solar collector.

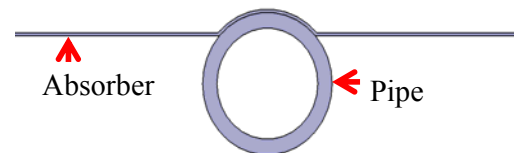


Figure-2. Schematic of the numerical model for the solar collector.

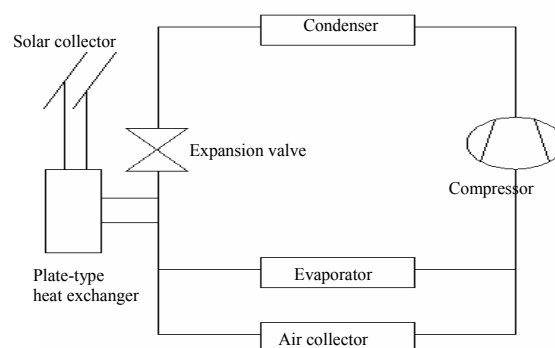


Figure-3. Schematic of the heat pump dryer with the solar collector and the air collector.

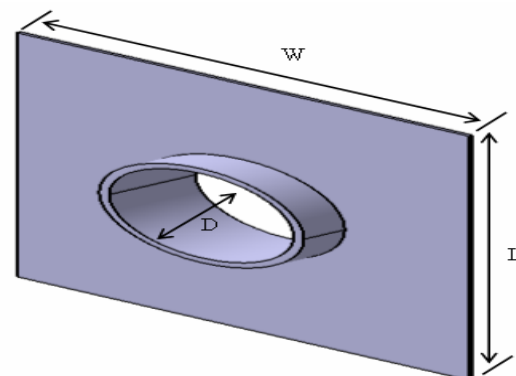


Figure-4. Schematic of the air collector fin module for conduction analysis.



variation between the inlet and outlet with the mass flow rate of the water. As the mass flow rate increases, the inlet-outlet temperature difference exponentially decreased while the heat absorption amount was constant, due to the adiabatic boundary conditions and sufficient residence time of the flow.

Although the inlet-outlet temperature difference is 15.3°C in the summer and 9.2°C in the winter when the mass flow rate is 0.0028 kg/s, they decrease to 0.7°C and 0.4°C, respectively, when the mass flow rate becomes 0.0563 kg/s. The heat absorption amounts for the summer and winter were found to be constants of approximately 180 W and 108 W, respectively, by assuming that the surfaces other than the absorber plate are

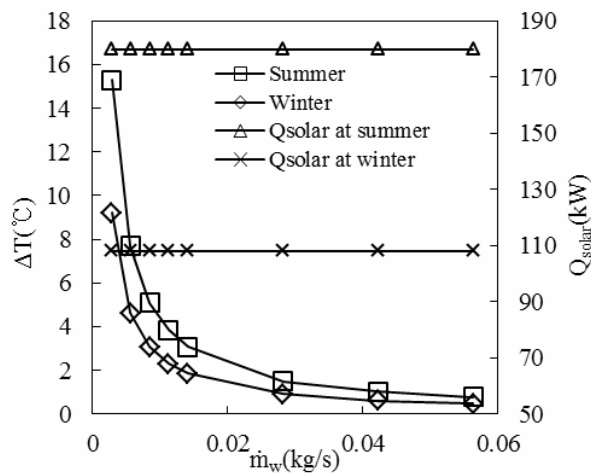


Figure-5. Variation of inlet-outlet solar collector temperature difference with the mass flow rate of water.

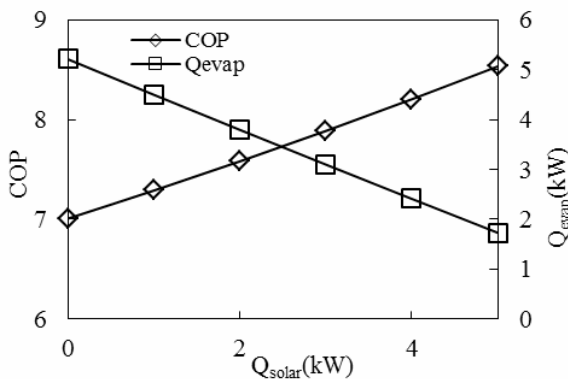


Figure-6. Variation of COP and evaporator heat absorption with the solar collector absorption heat for the dryer internal temperature of 0°C.

fully adiabatic. Therefore, when considering the entire solar collector, they become 1.62 kW and 0.97 kW, respectively. Such heat absorption can be increased by increasing the solar collector surface area, as they are proportional to each other.

Cycle analysis of the heat pump dryer with solar collector attached

In order to enhance the dryer performance in low temperatures, analysis was conducted while increasing the solar collector heat absorption. Figure-6 shows the COP and evaporator heat absorption variation according to the amount of solar collector heat absorption when the dryer internal temperature is 0°C. When only the internal evaporator was used, the COP was approximately 7 and the evaporator heat absorption amount was around 5.2 kW. When the amount of solar collector heat absorption was increased to a maximum of 5 kW, the internal evaporator heat absorption decreased to approximately 1.7 kW, so that the COP increased to approximately 8.5. Therefore, when the solar collector is used, not only the energy efficiency of the heat pump dryer increases but also the evaporator evaporating pressure increases, preventing the compressor liquid flood back phenomenon in low temperatures.

Figure-7 shows the mass flow rate and variation in condenser heat rejection with the solar collector absorption heat when the dryer internal temperature is 0°C. As the solar collector heat absorption increases, the mass flow rate of the refrigerant increases to a maximum of approximately 0.036 kg/s from approximately 0.027 kg/s. This is caused by the increase in evaporating pressure due to the solar collector heat absorption, increasing the refrigerant density at the compressor entrance and consequently increasing the refrigerant mass flow rate. Such refrigerant mass flow rate increase results in the increase of the condenser heat rejection from 6.0 kW to 7.6 kW, contributing to the reduction in drying time.

To investigate the dryer cycle at low temperature according to the amount of heat absorption when the solar collector is used, the P-h diagram is shown in Figure-8 for the dryer internal temperature of 0°C. For the standard cycle with no solar collector, the evaporating pressure and condensing pressure are 197 kPa and 445 kPa, respectively. The corresponding evaporating temperature is approximately

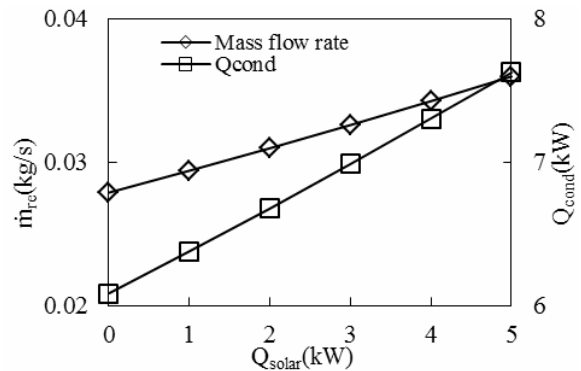


Figure-7. Variations of refrigerant mass flow rate and condenser rejection heat with the solar collector absorption heat for the dryer internal temperature of 0°C.

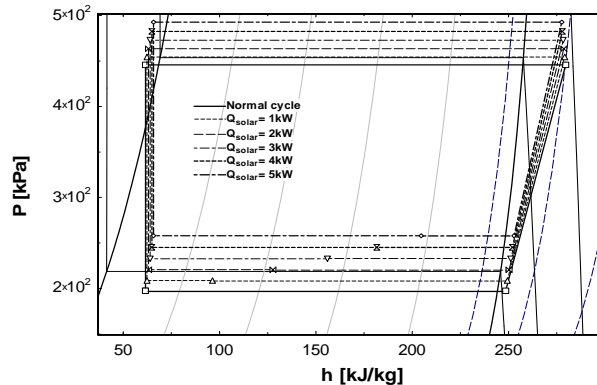


Figure-8. Variation of P-h diagram with the solar collector absorption heat for the dryer internal temperature of 0°C.

-10.4°C and there is a high probability of the liquid flood back phenomenon occurring due to the low dryer internal temperature of 0°C. However, when the solar collector absorption heat increases, the evaporating temperature and condensing pressure increase simultaneously, mitigating the phenomenon. When the solar collector heat absorption is 5 kW, the evaporating pressure and condensing pressure are 258 kPa and 492 kPa, respectively, and the evaporating temperature and condensing temperature are approximately -3.5 °C and 5 °C, respectively.

Cycle analysis of the heat pump dryer with air collector attached

Outside the drying chamber, a fin and tube type air collector, replacing the internal evaporator, was applied to the heat pump dryer. Figure-9 shows the variation in COP and evaporator heat absorption with the ambient temperature. Here, an internal evaporator was used for the ambient temperature of 0°C and an air collector was used for the ambient temperature of 10–30°C. When using the internal evaporator for 0°C ambient temperature, the COP was approximately 7.0 and the evaporator heat absorption amount was approximately 5.2 kW. When using the air collector for 10°C ambient temperature, the COP was approximately 8.5 and the heat absorption amount was around 6.7 kW, which are greater values than the COP and heat absorption amount when using the internal evaporator. Also, when the ambient temperature was 30°C, the COP increased to approximately 12.5 and the heat absorption amount also increased to 10.31 kW. Thus, at higher ambient temperatures, the air collector enhanced the dryer performance.

Figure-10 shows the variations of the refrigerant mass flow rate and condenser heat rejection with the ambient temperature when the air collector is used. The refrigerant mass flow rate and condenser heat rejection amount for an ambient temperature of 10°C were found to be approximately 0.036 kg/s and 7.62 kW, respectively. These are increases of approximately 0.008 kg/s and 1.6 kW for the refrigerant mass flow rate and condenser heat rejection, respectively, when compared to the case where the internal evaporator is used and the ambient

temperature is 0°C. Therefore, when the ambient temperature increases, the refrigerant mass flow rate and condenser heat rejection increase. When the ambient temperature is 30°C, the refrigerant mass flow rate and condenser rejection heat both increase to 0.055 kg/s and 11.2 kW, respectively, showing that significantly more heat can be obtained when compared to the case when the solar collector is used.

Figure-11 shows the variation of p-h diagram for the dryer using an air collector with ambient temperature. The evaporating pressure and condensing pressure are 258 kPa and 492 kPa, respectively, when using the air collector with an ambient temperature of 10 °C. These are increases of approximately 61 kPa and 47 kPa, respectively, when compared to the case where the internal evaporator is used and the ambient temperature is 0°C. This corresponds to the maximum heat absorption amount by the solar collector, and it is found that the evaporating pressure and condensing pressure can be increased further by using the air collector. When the ambient temperature is 30°C, the

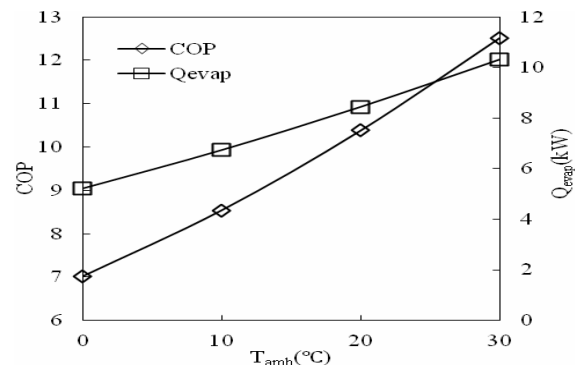


Figure-9. Variations of COP and evaporator absorption heat with ambient temperature when using the air collector.

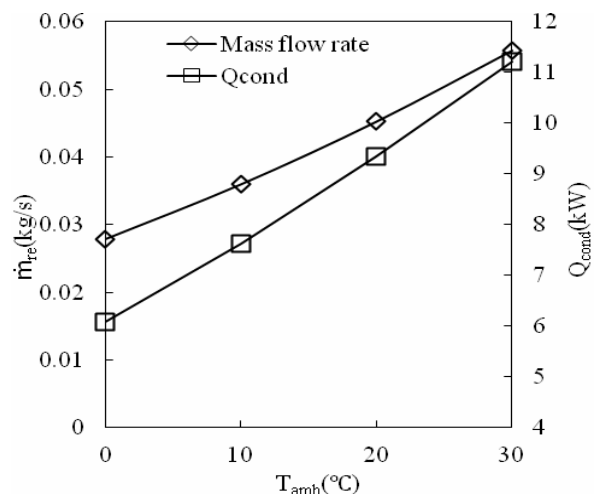


Figure-10. Refrigerant mass flow rate and condenser heat rejection amount variation according to the ambient temperature when the air collector is used.

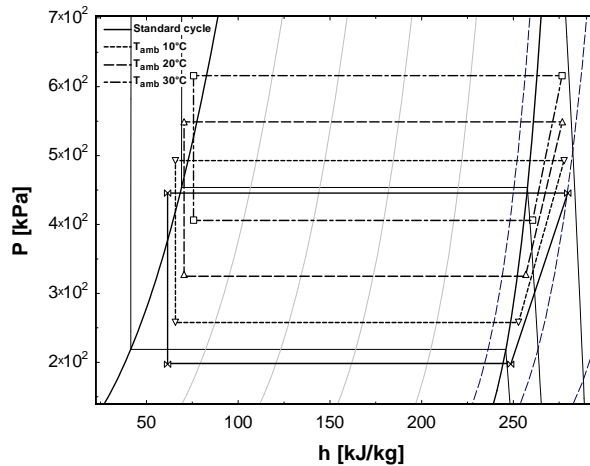


Figure-11. Variation of P-h diagram with the ambient temperature for the heat pump dryer with the air collector.

evaporating pressure and condensing pressure increase up to 403 kPa and 616 kPa, respectively, making it advantageous for enhancing the low temperature operation performance of the dryer. Meanwhile, a decrease in ambient temperature results in a decrease in the evaporating temperature, increasing the possibility of frost formation, and at an ambient temperature of 10°C, the evaporating temperature becomes approximately -3.5°C, leading to the possibility of frost formation if condensation occurs on the fin.

Condensation and frost in the air collector

If condensation and frost form on the air collector, the heat exchange efficiency decreases along with the decrease in the air collector efficiency. The previous results showed that when the ambient temperature is 10°C, the evaporating temperature decreases to approximately -3.4°C, increasing the possibility of condensation and frost occurrence. So, Figure-12 shows the conditions required for condensation to occur on the air collector fin according to the convective heat transfer coefficient for the ambient temperature of 10°C. Condensation does not occur at a relative humidity of 40% when the ambient temperature is 10°C and the convective heat transfer coefficient is 10 W/m²K. However, when the relative humidity becomes 45%, condensation occurs on the entire surface area, so there is a high possibility of frost formation due to the low temperature of below -2°C. In addition, condensation does not occur at the relative humidity is 40% for the ambient temperature of 10°C and convective heat transfer coefficient of 20 W/m²K. Also, when the relative humidity becomes 45%, condensation occurs partially, and when the relative humidity becomes 50%, condensation occurs on the entire surface area. In this case, since the maximum temperature on the fin was found to be about -0.9°C, there is a possibility of frost formation. When the convective heat transfer coefficient is 30 W/m²K, condensation does not occur at 40% relative humidity, but at 45%, it occurs

in proximity to the tube. However, when the relative humidity is 50%, condensation occurs on the entire fin.

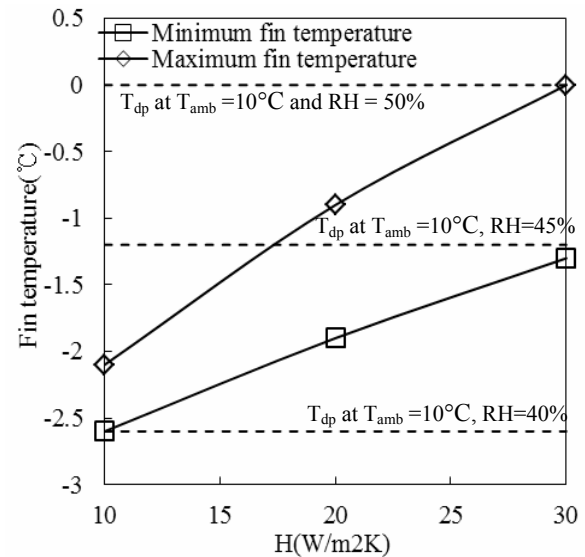


Figure-12. Conditions for condensation to occur on the air collector fin with the convective heat transfer coefficient at the ambient temperature of 10°C.

CONCLUSIONS

In this study, the following conclusions were obtained from the cycle analysis of the heat pump dryer with the solar collector and the air collector performed in order to improve the dryer's low temperature operating performance.

- The cycle analysis for the heat pump dryer with the solar collector revealed that the COP increases by 1.5 in comparison to the standard cycle when the solar collector heat absorption is further increased to 5kW. In addition, the evaporating pressure increases by approximately 61kPa, showing that the dryer performance at low temperature is improved.
- For the heat pump dryer with the air collector, the COP increases by 5.5 at the ambient temperature of 30°C in comparison to the standard cycle, showing that the air collector is superior to the solar collector. The condenser heat rejection and the evaporator heat absorption also increase by 5.2kW and 5.1kW, respectively, making it advantageous for improving the temperature elevation of the drying chamber and low temperature operability.
- When the ambient temperature is 10°C, the analysis of condensation and frost formation showed that frost formation can occur for the relative humidity of 45-50% and the convective heat transfer coefficient of 10-30 W/m²K.

In the future, an optimal combination of the solar collector and the air collector with varying operating conditions needs to be studied.



ACKNOWLEDGEMENTS

This research was supported by Basic Science Research Program through the National Research Foundation of Korea (NRF) funded by the Ministry of Education, Science and Technology (2011-0024805). In addition, this work was supported by the Human Resources Development program (No. 20134030200230) of the Korea Institute of Energy Technology Evaluation and Planning (KETEP) grant funded by the Korea Government Ministry of Trade, Industry and Energy.

Nomenclature

W = Width [mm]

L = Length [mm]

D = Diameter [mm]

\dot{m} = Mass flow rate [kg/s]

Q = Quantity of heat at evaporator [kW]

P = Pressure [kPa]

h = Enthalpy [kJ/kg]

T = temperature [°C]

COP = Coefficient of performance

ϵ = Heat exchanger effectiveness

C = Specific heat [J/kg°C]

H = Convective heat transfer coefficient [W/m²k]

RH = Relative humidity [%]

Subscripts

evap = Evaporator

sat = Saturation

air = Air

cond = Condenser

w = Water

re = Refrigerant

solar = Solar collector

dp = Dew point

amb = Ambient

REFERENCES

- [1] Bannister P., Carrington G and Chen G. 2002. Heat Pump Dehumidifier Drying Technology-Status, Potential and Prospects. Proc. of 7th IEA Heat Pump Conference. 1: 219-230.
- [2] Prasertsan S., Saen-Saby P., Prateepchaikul G and Ngamsritrakul P. 1996. Effects of Product Drying Rate and Ambient Condition on the Operating Modes of Heat Pump Dryer. Proc. of 10th Int. Drying Symp. A: 529-534.
- [3] Bivens D B., Allgood C C., Shiflett M B., Patron D B., Shely G S., Yokozeki A., Wells W D and Geiger K A. 1994. HCFC-22 Alternative for Air Conditioners and Heat Pumps. ASHRAE Transactions. 100(2): 566-572.
- [4] Cho H H., Ryu C G and Kim Y C. 2005. Experimental Study on the Cooling Performance of a Variable Speed CO₂ Cycle with Internal Heat Exchanger and Electronic Expansion Valve. Korean Journal of Air-Conditioning and Refrigeration Engineering. 17(3): 209-216.
- [5] Sarkar J., Bhattacharyya S and Gopal M. 2004. Natural Refrigerant-based Subcritical and Transcritical Cycles for High Temperature Heating. Int. Journal of Refrigeration. 30(1): 3-10.
- [6] Baek J., Groll E and Lawless P. 2005. Piston-Cylinder Work Producing Expansion Device in a Carbon Dioxide Cycle. Part I: Experimental Investigation. Int. Journal of Refrigeration. 28(2): 141-151.
- [7] Back N C., Lee J K., Kim H J., Yang Y S and Song B H. 2000. Experimental Study on the Solar Assisted Heat Pump System. Proceeding of Korean Solar Energy Society. 76-82.
- [8] Retkowski W. and Thoming J. 2014. Thermoeconomic optimization of vertical ground-source heat pump systems through nonlinear integer programming. Applied Energy. 114: 492-503.
- [9] Kim J., Park S R., Baik Y J., Chang K C., Ra H S., Kim M and Kim Y. 2013. Experimental study of operating characteristics of compression/absorption high-temperature hybrid heat pump using waste heat. Renewable Energy. 54: 13-19.